A Dual-Environment Active RFID Tag Antenna Mountable on Metallic Objects

Le Chang, Han Wang, Zhijun Zhang, *Fellow, IEEE*, Yue Li, and Zhenghe Feng, *Fellow, IEEE*

***Abstract*—A dual-environment active RFID tag antenna is proposed in this letter. A microstrip line fed at the middle portion is used to excite two operation modes under two different working environments. In free-space condition, the slot mode of the proposed antenna shows a 50-Ω load at the input port, while the patch mode shows a high impedance close to an open circuit. Therefore, only the slot contributes to radiation. In opposite, when the antenna is mounted on a conductive surface, the slot mode shows a high impedance at the input port, whereas the patch mode is matched and therefore radiates. A prototype of the proposed antenna is fabricated and tested. The measured impedance bandwidths are respectively 22.13% from 2.09 to 2.61 GHz and 4.17% from 2.35 to 2.45 GHz when the proposed antenna is respectively applied in free space and on a metallic surface. The measured peak gains and radiation efficiencies at 2.4 GHz in these two conditions are 4.13 dB and 93.2%, 9.21 dB and 95%, respectively. Good agreement between measurement and simulation demonstrates the feasibility of the dual-environment property.**

***Index Terms*—Patch antennas, RFID tags, slot antennas.**

I. Introduction

RADIO frequency identification (RFID) is a rapidly developing wireless technology that applies radio frequencies to exchange information between the readers and tags [1]. An RFID system consists of a tag, a reader, and a host. The tag, attached to the object, contains the information of the object. The communication link is established between the tag and the reader through magnetic field coupling or electromagnetic wave capturing according to operating frequency [2]. The reader collects data sent from the tag and transfers it to the host for the following processing. Due to its automatic wireless identification function, RFID systems have been widely applied. At low-frequency band (125–134 kHz), access control management is widely applied in a shopping mall; at high-frequency band (13.56 MHz), access cards and anticounterfeiting products are widely used in door security systems, bus cards, tickets, and so on; at ultrahigh-frequency band (433–960 MHz), real-time monitoring and logistics tracking are the main fields; at microwave frequency band (2.4 GHz, 5.8 GHz), the main application areas include electronic toll collection and other traffic controls. RFID systems can be classified into passive and active RFID systems according to whether the tags contain power sources.

The tags are attached to the surface of the objects, whose material properties determine the working environments for the tag antennas. The materials of the surfaces can be divided into two categories: low-conductivity materials and good conductors. The former indicates that the surfaces have no influence on the tag antennas, so this environment can be regarded as a free space. When a tag is attached to the metallic object such as a container, the impedance of the tag antenna may be greatly altered, leading to mismatch between the antenna and microchip. Moreover, the effect grows more severe with the increase of frequency. Therefore, the great challenge for the so-called dual-environment tags is how to apply them to the two aforementioned environments. Research works on the dual-environment tags have been explored in abundance [3]–[13].

Usually, the dual-environment tags contain a ground plane intrinsically to isolate the metallic objects. As for passive tags, the ground planes also play a very important role in conjugate matching between the tag antennas and the microchips. The impedances of microchips usually have a small real part ranging from 3 to 150 Ω and a large negative imaginary part between −50 to −200 Ω [3]. In order to realize conjugate matching, the locations of shorting vias were elaborately selected near the microchips [4]–[6]. A holeless dual-environment tag antenna was designed with folded dipole [7], whose impedance was adjusted by altering the dimensions of the parasitic patches. The planar inverted-F antenna (PIFA) was first used as the tag antenna mountable on different platforms by Hirvonen *et al.* [8], and then it was widely used as a dual-environment tag antenna owing to its intrinsically possessing ground planes [3], [9]. Dimensions of the slots were adjusted to alter the input impedances to apply these tags to different microchips [3], [9]. Chipsets for active RFID systems [10], [11] usually have a 50-Ω standard interface by using proper matching networks. Thus, the majority of the active tag antennas just need to match to 50 Ω [12]–[15], resulting in universality for active tags and convenience for antenna engineers. PIFAs were also widely adopted for dual-environment active tags [12], [13]. Disadvantages of these antennas were overcomplicated structures and poor radiation performances.

The working mechanisms of these dual-environment passive and active tags are placing ground plane layers in advance to shield any metallic objects. However, the tags will lose some performance if they are attached to low-conductivity objects, for example, antenna of the tag attached to a cardboard box is expected to have an omnidirectional beam. In this letter, a single-fed dual-environment active RFID tag antenna without any ground layers is proposed. The proposed antenna can be

Manuscript received September 16, 2015; revised November 23, 2015 and January 27, 2016; accepted February 6, 2016. Date of publication February 23, 2016; date of current version November 16, 2016. This work was supported by the National Basic Research Program of China under Contract 2013CB329002, the National Natural Science Foundation of China under Contract 61525104, and the China Postdoctoral Science Foundation funded project 2015T80084.

The authors are with the State Key Laboratory on Microwave, Tsinghua National Laboratory for Information Science and Technology, Department of Electronic Engineering, Tsinghua University, Beijing 100084, China (e-mail: changle4015@126.com; hanwang10@mails.tsinghua.edu.cn; zjzh@tsinghua.edu.cn; lyee@tsinghua.edu.cn; fzh-dee@mail.tsinghua.edu.cn).

Color versions of one or more of the figures in this letter are available online at http://ieeexplore.ieee.org.

Digital Object Identifier 10.1109/LAWP.2016.2533626

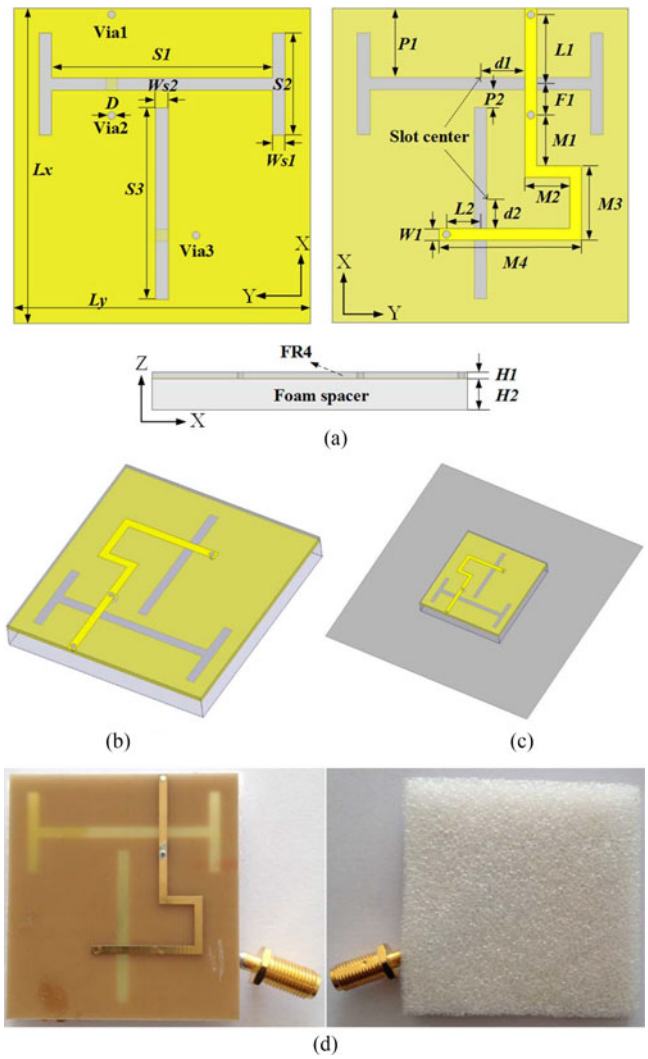

Fig. 1. (a) Configuration of the proposed antenna, (b) the free space, (c) metallic surface working environments, and (d) the antenna prototype.

applied in free space or on a metallic object owing to its dual-mode property. In different working environments, the proposed antenna supports one operation mode while suppressing the other. For free-space usage, the proposed antenna is operated in the slot mode and acquires an omnidirectional pattern. For the metal-object usage, the proposed antenna uses the metallic surface as its ground plane, leading to the patch mode operation. The dual modes are distinct from our previous work [16], where the dual modes include the dipole and patch modes. The antenna structure without any ground layers makes the tag compact, light, and convenient for usage. Measurement shows good performances under the two environments.

II. Antenna Design

The geometry of the proposed antenna is displayed in Fig. 1(a). The proposed antenna with a volume of $50 \times 47 \times 6$ mm^3 is composed of a meandered microstrip line, a slotted patch etched on an FR4 substrate ($\varepsilon_r = 4.4$, $\tan\delta = 0.02$), and a foam spacer. The patch with a horizontal H-shaped slot

TABLE I
Detailed Dimensions of the Proposed Antenna (Unit: Millimeters)

Parameter	Lx	Ly	S1	S2	S3	Ws1	Ws2	D
Value	50	47	35	16.2	30.5	2	2	1.2
Parameter	W1	F1	L1	L2	M1	M2	M3	M4
Value	1.8	5	11	5.4	7.9	9.1	11.8	22.5
Parameter	H1	H2	d1	d2	P1	P2		
Value	1	5	7.1	4.1	11	2.75		

and vertical slot is symmetrical about x-axis. The meandered microstrip line with its two ends shorted (via1 and via3) has a 50-Ω characteristic impedance. A coaxial cable with its inner conductor connected to the microstrip line and outer conductor connected to the patch through via2 is used to test the antenna. It is worth mentioning that the proposed antenna connects to the microchip in realistic application. The microstrip line crosses the two slots off center to excite two different operation modes under different working environments. The distances from the ends of the microstrip line to the two slots are respectively selected to obtain good impedance matching. The foam spacer with a height of 5 mm is used to create space between the patch and the metallic surface. A square ground plane with dimensions of 120×120 mm^2 is used to substitute the metallic surface. The size of the ground is selected freely, not an optimized result. Detailed dimensions of the proposed antenna are listed in Table I. The two working environments of the free-space and metallic-surface scenarios are illustrated in Fig. 1(b) and (c), respectively.

The design progress is illustrated in Fig. 2. The left column depicts the antennas evolution, the middle column shows the two working environments, and the right column illustrates the impedance curves of each intermediate antenna under different environments. The impedance curves of the free-space case are denoted by black dashed lines, while the metallic-surface cases by red solid lines. In addition, the impedance spots at 2.4 GHz are marked by red circles.

1) A rectangular patch fed by a 50-Ω end-shorted microstrip line (named Ant1) is shown in Fig. 2(a). A vertical slot is etched away to excite the patch. As illustrated in Fig. 2(b), when Ant1 is placed on the metal ground, by selecting the distance m_1 from the slot to the shorted end, Ant1 can be matched to 50 Ω. When Ant1 is applied in free space, it is mismatched and the port impedance is expected to be large enough, which can be viewed as the open circuit condition. By extending the distance l_1 from the slot to the port, impedance loci in Smith Chart rotate clockwise close to the circle edge, and the port impedance at 2.4 GHz is expected to be as close as possible to the open-circuit spot. In addition, the matching condition can be maintained attributed to the same characteristic impedance of the port and the microstrip line.
2) As shown in Fig. 2(c), an H-shaped slot is etched away from the patch (named Ant2) and another 50-Ω end-shorted microstrip line is used for feeding. As illustrated in Fig. 2(d), when Ant2 is applied in free space, by selecting the distance m_2 from the slot to the shorted end,

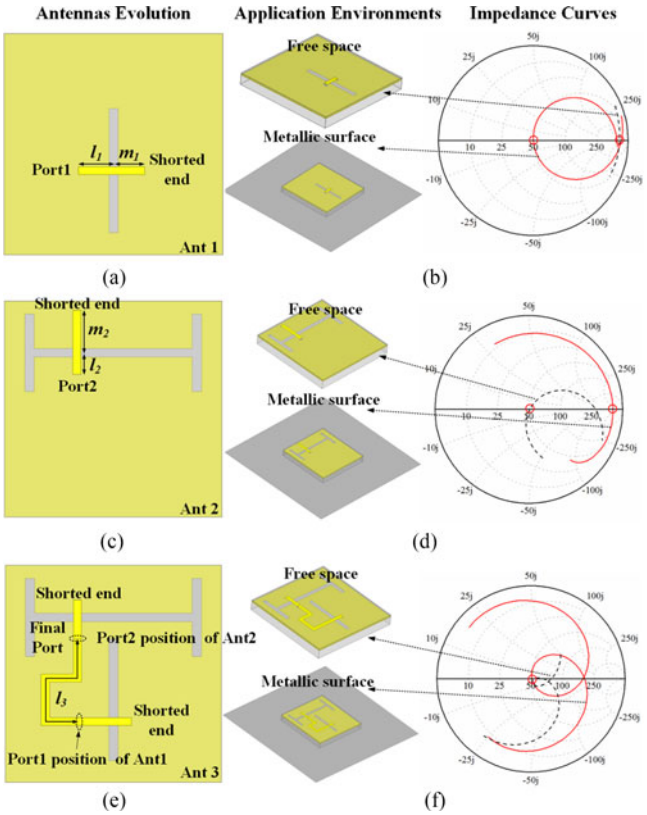

Fig. 2. Design steps of the proposed antenna. The left column depicts the antennas evolution, the middle column shows the two working environments, and the right column illustrates the impedance curves of each intermediate antenna under the two working environments. (The impedance spots at 2.4 GHz are marked by red circles.)

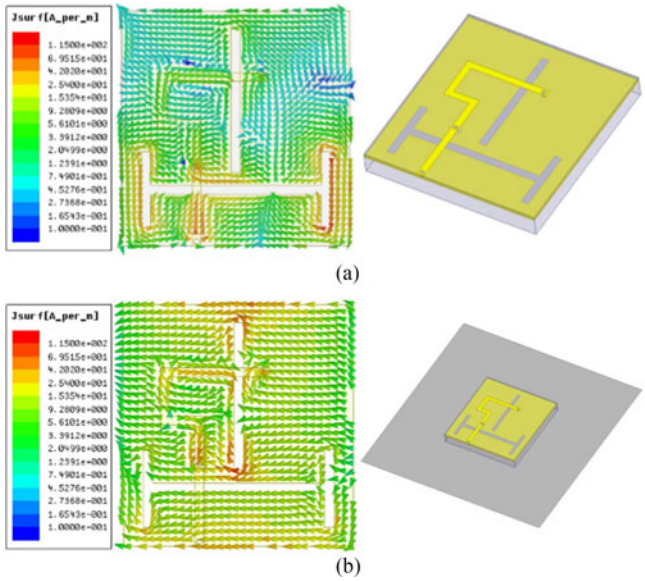

Fig. 3. Current distributions under the two environments. (a) Free-space case and (b) metallic-object case.

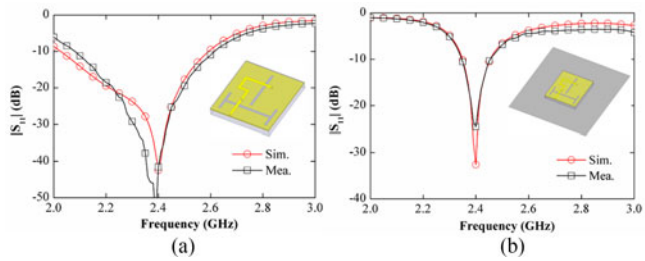

Fig. 4. Magnitude of the reflection coefficients under the two environments. (a) Free-space case and (b) metallic-object case.

Ant2 can be matched to 50 Ω. When Ant2 is placed on the metal ground, by extending the distance l_2 from the slot to the port, the port impedance at 2.4 GHz is expected to be as close as possible to the open-circuit spot.

3) Finally, the two slots should be etched away in the patch simultaneously and the two ports must be merged together. Because the two slots are orthogonal with each other, in each case, addition of one slot hardly affects the other. As the above principle stated, extending the microstrip line from the port1 for half substrate wavelength will simultaneously maintain the impedance characteristics under the two application scenarios. After elaborately selecting the trajectory and length of the extended line l_3 as shown in Fig. 2(e) (named Ant3), port 1 and port 2 are merged into one port. After some fine tunings, the impedance spots of the Ant3 under the two working environments are both matched to 50 Ω at 2.4 GHz as shown in Fig. 2(f).
4) The shorted ends are replaced by metallic via holes, and some fine tunings are necessary to constitute the finished antenna.

The current distributions at 2.4 GHz under the two working environments are displayed in Fig. 3. In free space, strong in-phase currents are concentrated at the two short edges of the H-shaped slot and the two x-direction edges of the patch, and they contribute to radiation. The orientation of the vertical slot aligns with the current direction, so the vertical slot has little impact on the slot mode. When the proposed antenna is applied on the metallic surface as shown in Fig. 3(b), it is a typical patch-mode current distribution. Meanwhile, the H-shaped slot aligns with the current direction, so it hardly affects the patch mode.

III. Antenna Fabrication and Measurement Results

The fabricated proposed antenna is shown in Fig. 1(d). The reflection coefficients measured in free space and on the metallic surface are shown in Fig. 4. As mentioned previously, the proposed antenna operates as a slot in free space. The measured impedance bandwidth ranges from 2.09 to 2.61 GHz (520 MHz, 22.13%), while the simulated result ranges from 2.03 to 2.59 GHz (560 MHz, 24.24%). The proposed antenna operates as a patch on the metallic surface. The measured impedance bandwidth is completely overlapped with the simulation, both ranging from 2.35 to 2.45 GHz (100 MHz, 4.17%).

When the proposed antenna are, respectively, working in free space and on a metallic surface, the normalized radiation patterns, peak gains, and radiation efficiencies are measured in an anechoic chamber. As for the free-space case, the corresponding E- and H-plane normalized patterns at 2.4 GHz are shown in Fig. 5(a) and (b), and the peak gains are shown in Fig. 6(a). It

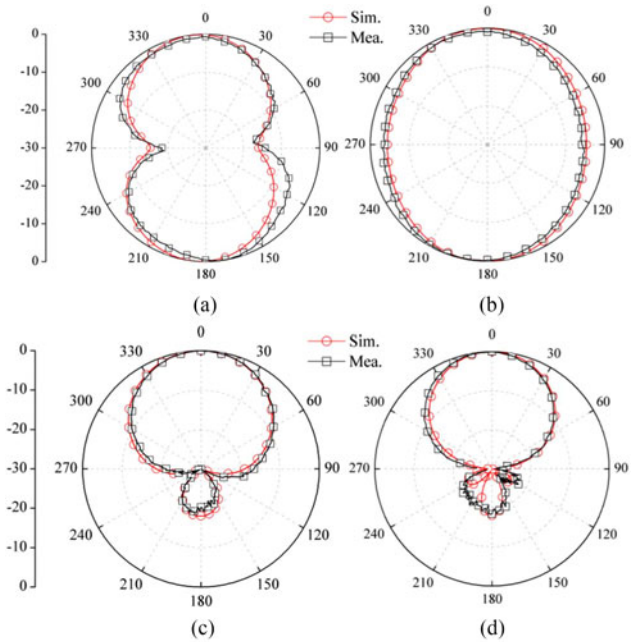

Fig. 5. Normalized radiation patterns under the two environments: (a) xz- and (b) yz-planes of the free-space case, and (c) xz- and (d) yz-planes of the metallic-object case.

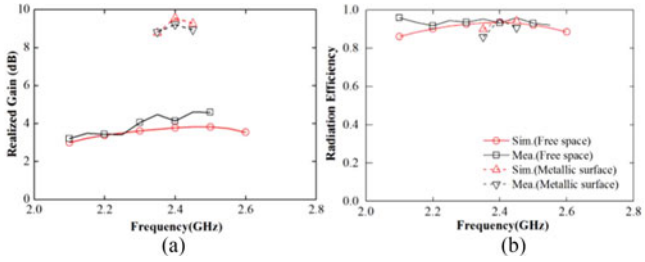

Fig. 6. (a) Peak gains and (b) radiation efficiencies under the two environments.

can be observed that the measured and simulated patterns agree well with each other, and the gains at 2.4 GHz are 4.13 dB in measurement and 3.77 dB in simulation. Compared to an H-shaped slot in an infinite ground, the peak gain is approximately 2 dB higher while the radiation patterns of the E- and H-plane are exchanged with each other. The reason is that the ground plane is finite. According to Fig. 3(a), the in-phase currents are along x-direction. More importantly, the tag antenna has an omnidirectional pattern in free space. Thus, the tag and the reader do not need to be aligned with each other. As for the metallic surface case, the normalized patterns of the H- and E-plane are shown in Fig. 5(c) and (d). They are the classic patch-mode patterns, and the measurement agrees well with the simulation. As observed from Fig. 6(a), the peak gains at 2.4 GHz are 9.21 dB in measurement and 9.54 dB in simulation. The measured peak gains and radiation efficiencies are displayed in Fig. 6. In free space, the measured peak gains and efficiencies, respectively, vary from 3.21 to 4.47 dB and 91.8% to 96%, while the simulated results from 2.99 to 3.82 dB and 86.12% to 93.46%. On the metallic surface, the measured peak gains respectively range from 8.82 to 9.21 dB and 85.90% to 95%, while the simulated results from 8.77 to 9.54 dB and 89.96% to 94.72%. The small deviation is caused by fabrication and measurement errors.

IV. Conclusion

The design of a dual-environment active RFID tag antenna is introduced in this letter. Due to its dual-mode property, the proposed antenna can operate in two different working environments. When it is attached to the objects with low conductivity materials, the situation can be considered as in free space. In this case, the port impedances of the H-shaped slot are matched and the patch is large enough, which can be viewed as the open-circuit condition, thus the antenna operates as the H-shaped slot. When the antenna is attached to the metallic object, there is a 5-mm height clearance between the tag and the metallic surface provided by the foam spacer. In this situation, the metallic surface acts as the ground plane, and the port impedances of the two modes flip, thus the proposed antenna operates as the patch. Good agreement between measurement and simulation verifies the feasibility of the design.

References

[1] K. Finkenzeller, *RFID Handbook* 2nd ed. New York, NY, USA: Wiley, 2004.
[2] P. Hajizadeh, H. R. Hassani, and S. H. Sedighy, "Planar artificial transmission lines loading for miniaturization of RFID printed quasi-yagi antenna," *IEEE Antennas Wireless Propag. Lett.*, vol. 12, pp. 464–467, 2013.
[3] H. Kwon and B. Lee, "Compact slotted planar inverted-F RFID tag mountable on metallic objects," *Electron. Lett.*, vol. 41, no. 24, pp. 1308–1310, Nov. 2005.
[4] B. Lee and B. Yu, "Compact structure of UHF band RFID tag antenna mountable on metallic objects," *Microw. Opt. Technol. Lett.*, vol. 50, no. 1, pp. 232–234, Jan. 2008.
[5] J. H. Lu and K. T. Hung, "Planar inverted-E antenna for UHF RFID tag on metallic objects with bandwidth enhancement," *Electron. Lett.*, vol. 46, no. 17, pp. 1182–1183, Aug. 2010.
[6] J.-H. Lu and G.-T. Zheng, "Planar broadband tag antenna mounted on the metallic material for UHF RFID system," *IEEE Antennas Wireless Propag. Lett.*, vol. 10, pp. 1405–1408, 2011.
[7] K. H. Kim, J. G. Song, D. H. Kim, H. S. Hu, and J. H. Park, "Fork-shaped RFID tag mountable on metallic surfaces," *Electron. Lett.*, vol. 43, no. 25, pp. 1400–1402, Dec. 2007.
[8] M. Hirvonen, P. Pursula, K. Jaakkola, and K. Laukkanen, "Planar inverted-F antenna for radio frequency identication," *Electron. Lett.*, vol. 40, no. 14, pp. 848–850, Jul. 2004.
[9] J.-S. Kim, W. Choi, and G.-Y. Choi, "UHF RFID tag antenna using two PIFAs embedded in metallic objects," *Electron. Lett.*, vol. 44, no. 20, pp. 1181–1182, Sep. 2008.
[10] TICC2510. (2015). [Online]. Available: http://www.ti.com.cn/cn/lit/ds/symlink/cc2510.pdf
[11] nRF24LE1. (2010). [Online]. Available: http://www.nordicsemi.com/eng/content/download/2443/29442/file/nRF24LE1_Product_Specification_rev1_6.pdf
[12] W. Choi, N.-S. Seong, J.-M. Kim, C. Pyo, and J. Chae, "A planar inverted-F antenna (PIFA) to be attached to metal containers for an active RFID tag," in *Proc. IEEE Int. Symp. Antennas Propag. Soc.*, 2005, vol. 1B, pp. 508–511.
[13] H. K. Ryu, S. Lim, and J. M. Woo, "Design of electrically small, folded monopole antenna using C-shaped meander for active 433.92 MHz RFID tag in metallic container application," *Electron. Lett.*, vol. 44, no. 25, pp. 1445–1447, Dec. 2008.
[14] L. Pazin, A. Dyskin, and Y. Leviatan, "Quasi-isotropic X-band inverted-F antenna for active RFID tags," *IEEE Antennas Wireless Propag. Lett.*, vol. 8, pp. 27–29, 2009.
[15] Z. Fang, R. Jin, and J. Geng, "Asymmetric dipole antenna suitable for active RFID tags," *Electron. Lett.*, vol. 44, no. 2, pp. 71–72, Jan. 2008.
[16] L. Chang, H. Wang, Z. Zhang, Y. Li, and Z. Feng, "Compact single-feed dual-environment antenna for active RFID tag application," *IEEE Trans. Antennas Propag.* vol. 63, no. 11, pp. 5190–5194, Nov. 2015.